M_{2n}	even Legendre functions of imaginary arguments
P_o	parameter defined by Eq. [1], A/cm$^{(1+\pi/2\beta)}$
P_{2n}	even Legendre polynomials
r	radial distance away from the electrode/insulator edge, cm
r_o	radius of the disk electrode, cm
r_q	radial position at which the potential is being determined, cm
R	universal gas constant, 8.3143 J/mol-K
S	stretching variable, cm^{-1}
T	absolute temperature, K
t, χ, z	complex coordinates
V	electrode potential, V
α_a, α_c	transfer coefficients
β	interior angle between insulator and electrode, radians
$\gamma(\chi)$	relates normal derivatives in original and transformed coordinate systems
δ	dimensionless average current density
$\epsilon^{(n)}$	nth coefficient in a perturbation series
η, ξ	rotational elliptic coordinates
κ	specific conductivity, Ω^{-1}cm^{-1}
π	3.141592654
ϕ	dimensionless solution potential
Φ	solution potential, V
Φ_o	solution potential adjacent to the electrode, V

Subscripts

as	asymptotic
avg	average
center	center of the disk electrode
edge	electrode/insulator interface
i, r	imaginary and real parts of a complex variable

Superscripts

p	primary
–	inner region variable
~	outer region variable

REFERENCES

1. A. C. West and J. Newman, *This Journal,* **136,** 2935 (1989).
2. M. E. Orazem and J. Newman, *ibid.,* **131,** 2857 (1984).
3. W. H. Smyrl and J. Newman, *ibid.,* **136,** 132 (1989).
4. A. C. West, Ph.D. Thesis, University of California, Berkeley, LBL-28076 (1989).
5. C. Wagner, *This Journal,* **98,** 116 (1951).
6. C. A. Brebbia, "The Boundary Element Method for Engineers," John Wiley & Sons, Inc., New York (1978).
7. B. D. Cahan, D. Scherson, and M. A. Reid, *This Journal,* **135,** 285 (1988).
8. J. Newman, *Ind. Eng. Chem.,* **60**(4), 12 (1968).
9. K. Nişancioğlu and J. Newman, *This Journal,* **121,** 523 (1974).
10. W. R. Parrish and J. Newman, *ibid.,* **117,** 43 (1970).
11. J. Newman, *ibid.,* **113,** 1235 (1966).
12. J. Newman, in "Electroanalytical Chemistry," A. J. Bard, Editor, pp. 187-351, Marcel Dekker, Inc., New York (1973).
13. M. Abramowitz and I. A. Stegun, Editors, "Handbook of Mathematical Functions," National Bureau of Standards, Washington, DC (1964).
14. L. Nanis and W. Kesselman, *This Journal,* **118,** 454 (1971).

Electrochemistry in Liquid SO_2

IX. Oxidation of n-Alkanes and Alkylammonium Ions at Pt Ultramicroelectrodes in Liquid SO_2

Edwin Garcia* and Allen J. Bard*

Department of Chemistry, The University of Texas at Austin, Austin, Texas 78712

ABSTRACT

When $CsAsF_6$ is used as the supporting electrolyte in liquid SO_2, the anodic solvent limit is about +6V *vs.* SCE. This very positive potential range allows the electrochemical oxidation of straight-chain hydrocarbons [C_nH_{2n+2} (n = 1-8)] and quaternary alkylammonium ions [R_4N^+ (R = $C_{2n}H_{2n+1}$, n = 3-16)] to be studied in this solvent system by cyclic voltammetry at Pt ultramicroelectrodes (10 and 25 μm). Single, totally irreversible, anodic voltammetric waves were observed. The peak potentials of these compounds became more negative with an increase in the length of the carbon chain. The peak potentials correlated with ionization potentials and the length of the carbon chain. Bulk electrolysis of n-hydrocarbons at low concentrations (1-5 m*M*) required 2 faradays per mole of hydrocarbon. However, when higher concentrations were employed (>10 m*M*), the electrolytic current did not fall to background levels. Some delocalization of the C σ—σ bonds is proposed to account for the negative peak potential shift with increasing length of the hydrocarbon chain.

We report here electrochemical studies of the oxidation of saturated hydrocarbons and alkylammonium ions in liquid SO_2. By using $CsAsF_6$ as supporting electrolyte, we have been able to study anodic processes to potentials equivalent to about +6V *vs.* SCE, an unprecedented positive potential range for such investigations. Since the initial reports of electrochemical oxidation of saturated hydrocarbons in nonaqueous media by Pletcher *et al.* (1-6), little attention has been devoted to this subject. This inactivity is perhaps due to the difficulties encountered in the study of normal alkane electrochemistry. For example, a medium where the very positive potentials needed to oxidize saturated hydrocarbons (>+2.0V *vs.* SCE) was not readily available during the initial studies. By employing quaternary ammonium salts of BF_4^- and PF_6^- as inert electrolytes in acetonitrile, nitroethane, propylene carbonate, and sulfolane, Pletcher *et al.* were able to obtain potentials up to *ca.* +3.0V *vs.* SCE. In these solvent systems C_nH_{2n+2} (where n = 5-10) was electrochemically oxidized with an overall stoichiometry of 2 faradays per mole (4). Totally irreversible electron transfers were observed for the oxidation of all saturated hydrocarbons studied. The carbocations thus produced underwent nucleophilic substitution with CH_3CN and CF_3CO_2H to generate the n-s-alkylacetamides and s-alkyltrifluoroacetates, respectively.

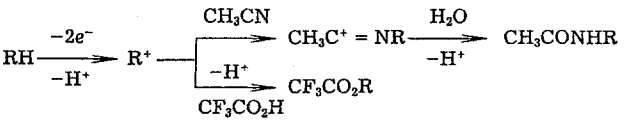

[1]

Other studies of C_5-C_{16} (17) and C_6-C_{10} (8) in neat and aqueous fluorosulfonic acids have been reported. With the exception of a recent report by Cassidy *et al.* (9) for electrochemical oxidation at an ultramicroelectrode, where CH_4 was reported to be oxidized, and a study by Bertram *et al.* (3), where protonated propane was oxidized in FSO_3H, no systematic study of the electrochemical oxidation of the shorter chain hydrocarbons (n < 5) has been reported.

* Electrochemical Society Active Member.

Recently, we have shown that potentials up to +4.7V *vs.* SCE were obtainable in liquid SO_2 with tetra-n-butylammonium hexafluoroarsenate ($TBAAsF_6$) as a background electrolyte (10). Thus, SO_2 appeared to be a useful solvent in which to study saturated hydrocarbon electrochemical oxidations. We have also demonstrated that the generation and isolation of stable compounds (with $E^{o\prime} > +3.0$V *vs.* SCE) is possible in this system and that the solvent limit is due to the oxidation of the electrolyte.

We report here the electrochemical oxidation of C_nH_{2n+2} (n = 1-8) with a decrease in peak potential with increasing number of carbon atoms in the paraffin chain. This peak potential shift is compared with a shift in $E_{1/2}$ observed for the oxidation of aromatic hydrocarbons (which has been attributed to an increase of π electron delocalization). Additional experimental data are cited and used to describe σ-delocalization in saturated hydrocarbons. Data are also presented for the oxidation of R_4N^+ (R = C_nH_{2n+1}, n = 3-16) which suggest that the background oxidation observed in $TBAAsF_6/SO_2$ solutions is caused by the oxidation of the alkyl chain of the TBA^+ ion.

Experimental

Solvent purification, preparation of ultramicroelectrodes, electrochemical measurements, and experimental procedures have been reported previously (10). Potentials were measured with respect to a Ag wire quasireference electrode and referenced to an aqueous saturated calomel electrode by assuming that the potential of the 9,10-diphenylanthracene (DPA)/DPA^+ couple is independent of solvent, as in previous studies in SO_2 (10). The reduction of SO_2 [forming $SO_2^{-\cdot}$ and consequently $S_2O_4^{=}$ (10)] was also used as an internal standard for potential scale calibration. This solvent reduction process is also a measure of the quasireference electrode, AgQRE, stability. Solutions of gaseous hydrocarbons, C_nH_{2n+2} (n = 1-3), were prepared by bubbling the gas through the electrolyte solution at −70°C using a gas dispersion tube (Ace Glass, coarse porosity, 25-50 μm) with vigorous stirring. Studies involving CH_4 were performed with a continuous gas flow while stirring the electrolyte solution. Voltammetric data were obtained shortly after the bubbling and stirring were stopped. The concentration of CH_4 could not be determined and was observed to change over time. The solubility of CH_4 is probably small at −70°C in SO_2 electrolyte solutions. The pressure above the solution was measured with a Hg manometer, and gas was added to the electrolyte solution until the desired pressure was obtained. Solutions of liquid hydrocarbons were prepared by adding the corresponding volume of liquid (*ca.* μl) to the solution with a microsyringe. Butane was first liquified at −70°C and the corresponding liquid sample drawn with a gas-tight syringe. Analysis of bulk electrolysis products from the oxidation of alkanes was done with a gas chromatograph (GC) (Hewlett-Packard 5890 with a 25m capillary column [bp-1], with a FID detector) and with a GC-mass spectrometer (GC-MS, Varian 3400-Finnigan MAT 700 ion trap detector).

Materials.—Methane (99.0%), ethane (99.0%), propane (99.0%), and butane (95.0%) were obtained from Linde (Union Carbide, NJ) and passed through activated alumina N-super I (ICN Biomedicals, Plainview, NY) on a glass wool column prior to use. Pentane (certified grade, Fisher Scientific, Fairlawn, NJ), hexane (99%, Phillips Petroleum, Bartlesville, OK), heptane (reagent grade, Spectrum Chemicals, Gardena, CA), and octane (97%, Phillips) were stored over activated alumina N-super I and degassed with dry N_2 prior to use.

Tetra-n-propylammonium hexafluoroarsenate ($TPAAsF_6$) was prepared by refluxing n-propyl bromide (reagent grade, MCB, Cincinnati, OH) under a dry nitrogen gas stream to which an equimolar amount of tri-n-propylamine (TPA, 98% Aldrich Chemical, Milwaukee, WI) was added dropwise. The resulting solid tetra-n-propylammonium bromide (TPABr) was dissolved in water to which aqueous lithium hexafluoroarsenate ($LiAsF_6$, Lithco, Bessemer City, NC) was added. $TPAAsF_6$, which precipitated from water, was redissolved in ethyl acetate to which 10% (v/v) diethyl ether was later added. This recrystallization was repeated twice and the salt was then dried at 120°C for 24h. The mp of the dried $TPAAsF_6$ was 235°-236°C.

Tripropyl-n-butylammonium hexafluoroarsenate ($TPBAAsF_6$) was similarly prepared from TPA and n-bromobutane (Fisher, certified grade). After drying *in vacuo*, the mp was 192°-194°C. The triethyl-n-pentyl, hexyl, and decylammonium hexafluoroarsenate salts ($TEPAAsF_6$, $TEHAAsF_6$, $TEDAAsF_6$, respectively) were synthesized from the corresponding alkyl bromides $C_5H_{11}Br$ 99%, $C_6H_{13}Br$ 98%, and $C_{10}H_{21}Br$ 98% (Aldrich Chemical), and triethylamine (98% J.T. Baker Chemicals, Phillipsburg, NJ) as described above. After vacuum drying the solids at 120°C for 24h, the mp were 286°C (dec, $TEPAAsF_6$), 184°C ($TEHAAsF_6$), and 176°C ($TEDAAsF_6$).

Trimethylcetylammonium hexafluoroarsenate ($TMCAAsF_6$) was prepared from aqueous solutions of trimethylcetylammonium bromide (TMCABr, 95%, Aldrich) and $LiAsF_6$. The product, purified as described above, had a mp of 208°-210°C (dec).

$CsAsF_6$ was prepared by addition of a solution of CsBr (Aesar, Johnson-Matthey, Seabrook, NH) to aqueous $LiAsF_6$. The precipitated $CsAsF_6$ was cold-filtered and redissolved in dimethylsulfoxide (DMSO; reagent grade, MCB, Norwood, OH) to which 20% (vol) CH_2Cl_2 (J.T. Baker, reagent grade) was added to precipitate the cesium salt. The $CsAsF_6$ obtained was practically insoluble in most nonaqueous aprotic solvents (such as MeCN, acetone, propylene carbonate, and ethyl acetate) but appreciably soluble in hot DMSO and DMF. The salt was thrice recrystallized from 90% DMSO/10% CH_2Cl_2 at −20°C; $CsAsF_6$ is insoluble in neat CH_2Cl_2. The resulting crystals were dried at 150°C for 48h and stored in a vacuum desiccator over $CaCl_2$.

Although the AsF_6^- salts (*e.g.*, $TBAAsF_6$, $TPAAsF_6$, and $CsAsF_6$) are nonhydroscopic, they slowly decompose to produce oxidizable products (at *ca.* +3.8V *vs.* AgQRE in SO_2) if not stored in a dry atmosphere. The salts that contain decomposition impurities were readily purified using the method previously described.

Results

Background processes.—$CsAsF_6$ was used as supporting electrolyte for the oxidation of methane, ethane, and propane. A typical cyclic voltammogram of the background current at a 25 μm Pt electrode in a 30 m*M* $CsAsF_6/SO_2$ solution at −30°C is shown in Fig. 1a. A saturated solution of $CsAsF_6$ in SO_2 at −70°C is approximately 30 m*M*. The anodic solvent limit is about 800 mV more positive (*ca.* 6V *vs.* SCE) than for SO_2 with $TBAAsF_6$ as supporting electrolyte. $TBAAsF_6$ could be used to study the longer chain hydrocarbons ($n \geq 4$) that oxidized at less positive potentials. Since $TBAAsF_6$ is more soluble than $CsAsF_6$, the solution resistance was smaller and less distortion was seen in the voltammograms. 25 μm Pt UMEs were used exclusively in $CsAsF_6/SO_2$ solutions, since voltammograms obtained with a 500 μm Pt electrode with $CsAsF_6$ were seriously distorted because of the large uncompensated solution resistance (*ca.* 10 MΩ).

Voltammetry of n-hydrocarbons.—Typical cyclic voltammograms (CV) for n-hydrocarbons at a Pt ultramicroelectrode (UME) (25 μm diam) and a larger Pt electrode (500 μm diam) are shown in Fig. 1b-d and 2, respectively. Only a single, totally irreversible, oxidation wave was seen for all hydrocarbons studied. Additional voltammetric waves were not observed when the potential sweeps were extended positive of the single irreversible oxidation peak, but the anodic solvent limit shifted to a less positive potential after addition of the alkanes. Note that the anodic current for the solvent oxidation did not reach a limiting value, even when the potential scan was extended to +11V *vs.* SCE (most of which is resistive drop in solution, $iR_{sol'n}$) where the current density was 0.12 A/cm² in 0.1*M* $TBAAsF_6$ electrolyte solutions. In a previous study (11) where the potential of a UME was scanned to potentials for the solvent reduction limit in neat nitrobenzene, the cathodic current density reached a limiting plateau of a few mA/cm². The large currents observed past the hydrocarbon voltammet-

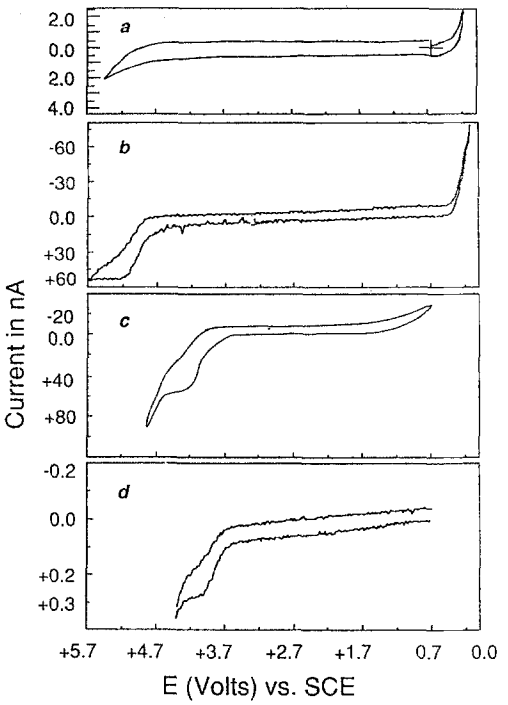

Fig. 1. Cyclic voltammograms for n-hydrocarbons at a 25 μm diam Pt ultramicroelectrode (UME) at −70°C in liquid SO_2: (a) background of 30 mM $CsAsF_6$, v = 1 V/s; (b) 1 atm methane in 30 mM $CsAsF_6$, v = 5 V/s; (c) 50 mM pentane in 0.2M $TBAAsF_6$, v = 100 V/s; and (d) 10 mM hexane in 0.2M $TBAAsF_6$, v = 10 V/s.

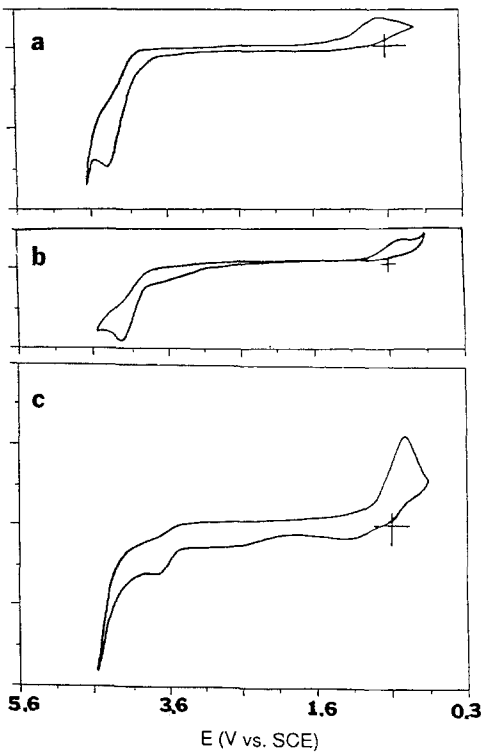

Fig. 2. Cyclic voltammograms for n-hydrocarbons at a 500 μm diam Pt electrode at −70°C in liquid SO_2: (a) 50 mM butane in 0.2M $TBAAsF_6$, v = 10 V/s, S = 0.5 μA; (b) 10 mM pentane in 0.2M $TBAAsF_6$, v = 5 V/s, S = 10 μA; and (c) 10 mM heptane in 0.2M $TBAAsF_6$, v = 10 V/s, S = 20 μA.

ric peak are attributed to the oxidation of the alkylammonium supporting electrolyte. When similar concentrations of electrolyte and n-alkane are used (10 m*M* $TBAAsF_6$ and n-heptane), two voltammetric waves were observed. Oxidation of quaternary ammonium ions in SO_2 will be described elsewhere.

When fast scan rates, v, up to 10 kV/s were used in an attempt to obtain reverse cathodic waves of the primary oxidation, none were observed. A summary of the cyclic voltammetric data for the oxidation of several hydrocarbons is given in Table I. The large variation observed in the peak current for CH_4 oxidation reflects our inability to maintain a constant concentration for replicate experiments. Although this case is by far the worst, similar problems were observed with the other gaseous hydrocarbons. This concentration variation, which affected the magnitude of the i_{pa}, did not substantially affect the peak potentials observed. The anodic peak potential, E_{pa}, became less positive as the length of the carbon chain increased. A summary of E_{pa} values for all of the alkanes studied, at v = 10 V/s, is shown in Table II.

The cathodic wave shown in Fig. 2, at about +0.7V *vs.* SCE, is attributed to the reduction of H^+. A similar reduction wave was observed (at +0.7V *vs.* SCE) when a mixture of CF_3COOH/acetic anhydride (90/10% v/v) was added to a SO_2 solution of the electrolyte. These reduction waves on reverse scan are not seen in Fig. 1b-d (for UMEs), because the rapid hemispherical diffusion at the smaller electrodes causes products to be carried away rapidly from the vicinity of the electrode surface (12-15). These reduction waves were observed at the UMEs when the scan rate was increased to >20 V/s.

Coulometric studies.—Controlled potential (bulk) electrolysis of the short chain hydrocarbons ($n < 4$), which required the more positive potentials obtained only in $CsAsF_6$, could not be carried out at larger electrodes because of the large uncompensated resistance of this system (*ca.* 10 MΩ). Frequent overloading of the potentiostat during electrolysis was observed when large electrodes

Table I. Voltammetric data for the oxidation of alkanes in sulfur dioxide at −70°C

Scan rate (V/s)	Methane[a]						Heptane[c]			
	Exp. 1[b]		Exp. 2[b]		Exp. 3[b]		10 m*M*[d]		14 m*M*[b]	
	i_{pa}	E_{pa}	i_{pa}	E_{pa}	i_{pa}	E_{pa}	i_{pa}	E_{pa}	i_{pa}	E_{pa}
0.01							1.87	3.48		
0.02							2.38	3.48		
0.05							2.50	3.41		
0.1	3.25	4.46	1.29	4.80			3.25	3.47	1.15	3.79
0.2	4.00	4.46	1.41	4.81			5.88	3.51	1.40	3.66
0.5	5.75	4.56	1.82	4.84			7.75	3.62	2.00	3.62
1.0	7.69	4.70	2.49				12.1	3.72	2.35	3.64
2.0	9.00	4.85	3.43	5.02					2.65	3.82
5.0	12.00	5.04	4.29	5.02	1.64	5.14			3.30	3.84
10			4.45	5.16	1.54	5.23	21.3	3.91	3.65	3.85
20		5.14	4.88	5.26	1.64	5.41				
50		5.59	5.98	5.40	2.09	5.74				

[a] 1 atm of methane above electrolytic solution, obtained with a 25 μm Pt UME.
[b] i_{pa} = anodic peak current (in μA), E_{pa} = anodic peak potential (V *vs.* SCE, ±10 mV).
[c] Obtained at a 100 μm Pt electrode.
[d] i_{pa} = anodic peak current (in 100 nA).

Table II. Anodic peak potentials for alkanes and ammonium ions in SO_2 at −70°C[a]

Species	Anodic peak[f] potential *vs.* SCE
Alkanes	
Methane[b]	+5.10
Ethane[b]	+4.73
Propane[b]	+4.57
n-Butane[c]	+4.52
n-Pentane[c]	+4.26
n-Hexane[c]	+4.15
n-Heptane[c]	+3.97
n-Octane[c]	+3.97
Alkylammonium ions[d]	
Tetraethylammonium[b]	+5.27
Tetra-n-propylammonium[b]	+5.18
Tetra-n-butylammonium[e]	+4.93
n-Pentyltriethylammonium[c]	+4.72
n-Hexyltriethylammonium[c]	+4.52
n-Decyltriethylammonium[c]	+3.98
Cetyltrimethylammonium[c]	+3.82

[a] Obtained with a 25 μm diam Pt UME at 10 V/s.
[b] $CsAsF_6$ was used as supporting electrolyte.
[c] $TBAAsF_6$ was used as supporting electrolyte.
[d] Counterion was AsF_6^-.
[e] $TEAAsF_6$ was used as electrolyte.
[f] Instrumental error ≤ 10 mV.

were used in this solvent system, indicating that the available output voltage (100V) was insufficient to control the electrode at the imposed potential. Attempts to improve the conductivity of the $CsAsF_6/SO_2$ solutions by increasing the solution temperature were not successful (16). We thus conclude that large electrodes, used for voltammetry and bulk electrolysis, will be difficult to use in $CsAsF_6/SO_2$. Electrolyses of the hydrocarbons that oxidized at potentials negative of *ca.* +4.5V *vs.* SCE (C_nH_{2n+2} [where n = 4-7]) were carried out in a 0.2*M* $TBAAsF_6/SO_2$ solution. When 5.38 m*M* butane (at 4.7V), 3.82 m*M* pentane (at 4.4V), 3.04 m*M* hexane (at 4.3V), or 4.10 m*M* heptane (4.2V) were electrolyzed at −70°C, the number of faradays per mole, n_{app}, was found to be *ca.* 2; the experimental data from the electrolyses are summarized in Table III. When larger concentrations of the hydrocarbons were used (10-100 m*M*), more than 5 faradays per mole were consumed at the point where the current had decayed to about 50% of its initial value. The dependence of n_{app} on the concentration of hydrocarbon will be discussed later.

One ml gas samples were obtained with a 5 ml gas-tight syringe above the solution (at −30°C) throughout the electrolysis of a solution of 0.1*M* pentane and 0.2*M* $TBAAsF_6$ in liquid SO_2. The controlled potential electrolysis was carried out at +4.4V *vs.* SCE. Five chromatographic peaks were observed with the flame ionization detector (FID). Samples of normal, branched, and cyclic hydrocarbons were used as comparative standards (1 μl of the liquid and 1 ml of gaseous samples were injected to calibrate to BP-1 column), and peaks were identified as: (*i*) pentane (68.7%), (*ii*) butane (23.8%), (*iii*) 2-methyl butane (3.8%), (*iv*) 1-pentene (2.3%), and (*v*) 2-methyl-1-pentane (1.4%). Because SO_2 does not ionize in the flame of the FID, an SO_2 peak was not detected.

Table III. Summary of coulometric data for the oxidation of alkanes in SO_2[a]

	Butane	Pentane	Hexane	Heptane
Concentration (m*M*)	5.38	3.82	3.04	4.10
Coulombs measured	32.7	25.7	19.3	27.1
Coulombs for n_{app} = 2	34.5	25.7	19.9	27.4
Initial current (mA)	1.13	0.48	0.37	0.51
Final current (μA)	11.5	4.74	1.85	5.31
Electrolysis time (h)	4.7	3.8	3.1	4.3
Faradays/mol	1.80	1.99	1.88	1.96

[a] Obtained with 2 cm^2 Pt gauze electrode in 35 ml of 0.2*M* $TBAAsF_6$.

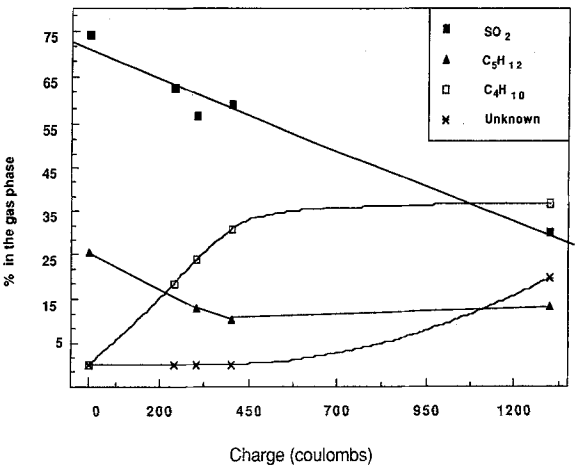

Fig. 3. Product appearance in the gas phase above a 10 m*M* pentane/0.2*M* $TBAAsF_6$ solution at −70°C in liquid SO_2 as a function of electrolysis charge during electrolysis at a Pt electrode (2 cm^2) at 4.4V *vs.* SCE.

When the same sample was analyzed by GC-MS (ion trap), only four chromatographic peaks were resolved from the gas above the electrolytic solution. These peaks were identified by comparison with library mass spectra. The relative percentage of these compounds as a function of amount of charge passed during the electrolysis is shown in Fig. 3. These compounds were identified as SO_2, pentane, and butane. A reasonable fit was not obtained for the fourth component of the mixture. Similarly, when n-heptane was electrolyzed, the major components in the gas above the electrolytic solution by GC were hexane (53.7%), pentane (29.2%), and methane or ethylene (17.1%).

Because SO_2 appears as the predominant peak at the GC-MS detector (thermocouple), the SO_2 peak will mask peaks of products that have similar retention times. Therefore, the differences in the number of chromatographic peaks seen for GC and GC-MS do not reflect differences in product distribution but are probably caused by the difference in detector response.

Voltammetry of tetra-alkylammonium ions.—Our previous studies (10) showed that the anodic limiting process in liquid $SO_2/TBA^+AsF_6^-$ was due to the oxidation of the supporting electrolyte. Thus, by using $CsAsF_6$ as a supporting electrolyte, the oxidation of tetra-alkyl ammonium ions can be investigated. Typical CVs of some tetra-alkylammonium salts are shown in Fig. 4. A single, totally irreversible anodic wave was observed for all of the salts studied. A corresponding reverse cathodic wave was not observed for scan rates up to 1000 V/s; at higher scan rates, the charging current obscured the faradaic current. As seen in Fig. 4, the peak potentials became less positive as the length of the alkyl chain on the ammonium ion increased, similar to the trend observed for the saturated hydrocarbons. For ex-

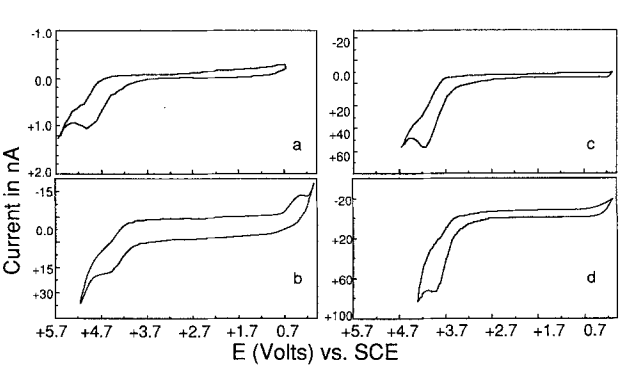

Fig. 4. Oxidation of ammonium ions at a 25 μm Pt UME in 30 m*M* $CsAsF_6$ solution at −70°C: (a) 2 m*M* $TBAAsF_6$, v = 10 V/s; (b) 5 m*M* $HTEAAsF_6$, v = 10 V/s; (c) 10 m*M* $DTEAAsF_6$, v = 10 V/s; and (d) 15 m*M* $CTEAAsF_6$, v = 10 V/s.

ample, the E_{pa} of TPA^+ was 80 mV more positive than that of TBA^+ (tetra-n-propyl and tetra-n-butylammonium, respectively). As the alkyl chain was increased further, the peak potential continued to shift, reaching about +3.8V *vs.* SCE for $TMCA^+$ (trimethylcetylammonium cation) in which the longest carbon chain contains 16 carbons. In all cases the E_{pa} for the alkylammonium ion was more positive than that of the corresponding hydrocarbon. Peak potential data obtained at 10 V/s for six different alkylammonium salts are summarized in Table II. Characteristic voltammetric data is summarized in Tables IV and V.

The voltammetry of tetramethylammonium hexafluoroarsenate (TMA^+AsF_6) was attempted, but no waves were observed, because residual water present in the electrolyte, even when the salt was dried under vacuum, produced anodic current in the region where a wave for the oxidation of TMA^+ was expected.

Discussion

Reaction mechanism.—While the cyclic voltammetric results clearly demonstrate that oxidation of normal alkanes is possible in SO_2 solutions, the usual data treatment [dependence of peak current and peak potential on scan rate (17, 18)] could not be used to establish a reaction mechanism. Thus, the mechanism(s) we tentatively propose are largely speculative. The apparent number of electrons involved in the oxidation of alkanes can be estimated roughly from the anodic peak current (19) (Tables I and V), assuming a value for the diffusion coefficient of 3.3×10^{-6} cm^2/s (20). This apparent number of electrons, n, decreased with increase in scan rate approaching two at low alkane concentrations (heptane, 14 m*M*). For larger concentrations (hexane and heptane), n was larger than two. The bulk electrolysis data, obtained at low concentrations of the alkanes in liquid SO_2, agrees with the results of Clark *et al.* (4) of an overall reaction mechanism involving 2 faradays per mole. These authors proposed that the electrochemical oxidation of normal alkanes in nucleophilic solvents like MeCN occurs via an ECE reaction mechanism (1-6). After the initial electrochemical oxidation, in which alkane radical cations are formed, a rapid loss of a proton follows. The radical species that forms ($R\text{-}CH_2\cdot$) is oxidized further to form a carbonium ion ($R\text{-}CH_2^+$) that undergoes solvent nucleophilic substitution (forming in MeCN on N-s-alkylacetamide, $R\text{-}CH_2CONHR$) (Eq. [1]).

Although the electron stoichiometry in SO_2 is also 2 faradays per mole, the fate of the cation formed differs from that reported in other solvents (1-6). Because SO_2 is at best a weak nucleophile, and AsF_6^- is a noncoordinating anion (21), nucleophilic substitution of the alkane cation by the solvent or supporting electrolyte is unlikely. Because the electrolytic current did not decay to background levels, secondary reactions (*e.g.*, deprotonation of the cation) or reaction with neutral alkanes could occur during the electrolysis of concentrated n-alkane solutions. These secondary reactions would generate products that oxidize at less positive potentials than the starting materials. For example, the oxidation of pentane would generate pentane cations which would react with neutral pentane to form decane. Decane would, in turn, be oxidized, adding to the overall observed current, and hence the electrolytic current would not decay exponentially as expected (19a). Alternatively, the intermediates could be sufficiently strong oxidants to cause some oxidation of SO_2 or the electrolyte in a catalytic (EC′) route (19).

The analysis of the oxidation products by GC and GC-MS showed no evidence of C—C bond formation, but rather suggested that after oxidation in dilute solutions, the alkane cation radical loses a carbon atom to form an n-1 alkane. For example, oxidation of heptane produced mostly hexane, and oxidation of pentane, mostly butane. In general, alkanes with one less carbon ($n - 1$) were the major product observed in the gas phase for the oxidation of alkanes with five or more carbons. If the chemical reactions of the shorter alkanes is similar to that of the longer ones, the oxidation products would also be mostly $n - 1$

Table IV. Voltammetric data for the oxidation of pentyltriethylammonium in sulfur dioxide at −70°C[a]

Scan rate (V/s)	20 m*M*[b]		5 m*M*[b]		5 m*M*[c]	
	i_{pa}	E_{pa}	i_{pa}	E_{pa}	i_{pa}	E_{pa}
5.0	407	4.71				
10	524	4.72	252	4.72	46.3	4.70
20	720	4.83	363	4.75	49.8	4.70
50	926	5.12	479	4.84	61.3	4.73
100	963	5.10	655	4.87	76.3	4.76
200	910	5.40	1010	4.88	77.1	4.83
500	696	6.10	2000	4.95	86.0	4.91
1000		6.09				

[a] Obtained in 0.20*M* $TEAAsF_6$. i_{pa} = anodic peak current (nA), E_{pa} = anodic peak potential (V *vs.* SCE, ±10 mV).
[b] Obtained with a 25 μm diam Pt UME.
[c] Obtained with a 10 μm diam Pt UME.

Table V. Voltammetric data for the oxidation of ammonium ions in sulfur dioxide at −70°C[a]

Scan rate (V/s)	Hexyltriethylammonium+[b]		Decyltriethylammonium+[c]		Cetyltrimethylammonium[c]	
	i_{pa}	E_{pa}	i_{pa} (μA)	E_{pa}	i_{pa} (μA)	E_{pa}
0.1					1.16	3.50
0.2					1.60	3.53
0.5					1.83	3.55
1.0			5.50	3.87	2.73	3.60
2.0			7.76	3.89	5.72	3.74
5.0			11.1	3.89	6.15	3.80
10	63	4.52	11.3	3.99	9.67	3.82
20	84	4.52			13.0	4.00
50	128	4.53		3.98		
100	218	4.54				
200	234	4.58				

[a] Obtained in 0.20*M* $TBAAsF_6$.
[b] Obtained with a 25 μm diam Pt UME.
[c] Obtained with a 0.5 mm diam Pt electrode.
i_{pa} = anodic peak current, E_{pa} = anodic peak potential (V *vs.* SCE, ±10 mV).
Hexyltriethylammonium AsF_6 = 10 m*M*.
Decyltriethylammonium AsF_6 = 1 m*M*.
Cetyltrimethylammonium AsF_6 = 5 m*M*.

products. The reaction products for methane oxidation are unknown. To the best of our knowledge, this apparent clipping of atoms off an alkane chain has not been previously observed and more closely resembles the fragmentation observed in mass spectrometry upon ionization in the gas phase, where typical reactions would be

$$\text{R-CH}_2\text{-CH}_2\text{-CH}_2\text{-CH}_3^{+\cdot} \begin{cases} \longrightarrow \text{R-CH}_2^{\cdot} + \text{CH}_2\text{-CH}_2\text{-CH}_3^{+} \\ \longrightarrow \text{R-CH-CH}_2^{\cdot} + \text{CH}_2\text{-CH}_3^{+} \\ \longrightarrow \text{R-CH}_2\text{-CH}_2\text{-CH}_2^{\cdot} + \text{CH}_3^{+} \end{cases} \quad [2]$$

Unsaturated hydrocarbons were also produced (*e.g.*, 1-pentene from pentane oxidation) during electrolysis, but these represented only a small fraction of the products. Because unsaturated and branched hydrocarbons oxidize at less positive potentials than n-alkanes, a smaller amount of these is expected to be detected in the gas above the solution as they would be preferentially oxidized.

The reduction of protons, observed at *ca.* +0.7V *vs.* SCE (Fig. 2) after the voltammetric oxidation of the alkanes, suggests a similar mechanism to that of previous studies (1-6) where proton loss followed the initial oxidation. Based on the voltammetric and coulometric data presented here, the overall reaction mechanism for the oxidation of alkanes would be of an ECEC type

$$\text{R-CH}_2\text{CH}_3 \overset{\text{E}}{\rightleftharpoons} \text{R-CH}_2\text{-CH}_3^{+\cdot} + e^- \quad [3]$$

$$\text{R-CH}_2\text{CH}_3^{+\cdot} \xrightarrow{\text{C}} \text{R-}\dot{\text{C}}\text{H-CH}_3 + \text{H}^+ \quad [4]$$

$$\text{R-}\dot{\text{C}}\text{H-CH}_3 \overset{\text{E}}{\rightleftharpoons} \text{R-}\overset{+}{\text{C}}\text{H-CH}_3 + e^- \quad [5]$$

In dilute solutions the second chemical step could be the loss of a CH_3^+ (possibly by reaction with solvent or AsF_6^-) to generate an $n - 1$ alkane radical that could react with available protons to form the corresponding alkane cation (Eq. [6]). Note, however, that products containing sulfur, oxygen, fluorine, and/or arsenic were not detected in the gas above the electrolytic solution, although some could be present in the liquid as less volatile products

$$\text{R-}\overset{+}{\text{C}}\text{H-CH}_3 \rightarrow \text{R-}\ddot{\text{C}}\text{H} + \text{CH}_3^+ \quad [6]$$

Another possibility for a second chemical step could include the further loss of protons with formation of an olefin (Eq. [7] and [8]).

$$\text{R-}\overset{+}{\text{C}}\text{H-CH}_3 \rightarrow \text{R-}\ddot{\text{C}}\text{H} - \text{CH}_2 + \text{H}^+ \quad [7]$$

$$\text{R-}\ddot{\text{C}}\text{H-CH}_2 \rightarrow \text{R-CH} = \text{CH}_2 \quad [8]$$

Effect of chain length on E_{pa}.—Although the shift in peak potential with increasing length of the hydrocarbon chain has been previously observed (1-9), no explanation for it has been proposed. This trend is analogous to the $E_{1/2}$ shift toward less positive potentials found with aromatic hydrocarbons as the extent of conjugation increases, *e.g.*, in the series: benzene, naphthalene, anthracene, and tetracene (Fig. 5a). Oxidation of these aromatic hydrocarbons, via loss of electrons from the highest occupied molecular orbital (HOMO), becomes easier with increasing delocalization of the π system (22). The $E_{1/2}$ is thus shifted toward less positive potentials with increasing molecular size. Similarly, we propose σ delocalization to account for the peak potential shift observed for increasing chain length in the n-alkanes.

A correlation of the ionization potential *vs.* peak potential and HOMO energies (22) for normal hydrocarbons is shown in Fig. 5b. The correlation coefficient obtained from a least squares linear fit was 0.98. Some deviation from linearity is expected, both because the peak potential for an irreversible electron transfer is not a thermodynamic quantity and depends on the rate of the chemical reaction which follows oxidation, and because the extent of solvation energy of the resulting radical cations is probably a function of chain length. Similar problems arise in correlations of the $E_{1/2}$ values for the oxidation of aromatic hydrocarbons in solvents in which the radical cations are unstable (22). Because of the following reaction of the radical

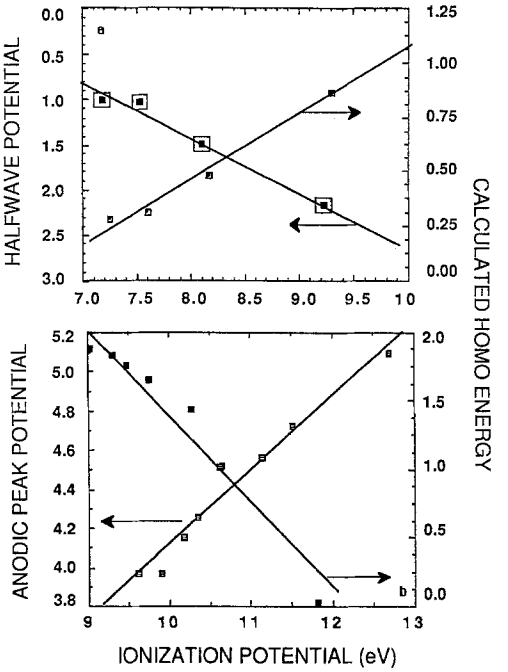

Fig. 5. (a) Correlation of $E_{1/2}$ (in MeCN), and energy of the HOMO (22) *vs.* the gas-phase ionization potential for aromatic hydrocarbons (22). (b) HOMO *vs.* the gas-phase ionization potential for saturated hydrocarbons.

cation, the anodic peak potential will be negative of the thermodynamic $E^{\circ\prime}$, to an extent that depends on the rate of the following chemical reaction, which is probably not the same for different hydrocarbons. For the oxidation of methane and heptane, the observed peak potential shift (Table I) ranged from 400 to 78 mV per tenfold change in scan rate. If one assumes an E_rC_i reaction mechanism (19b), an 18 mV shift is predicted for a one-electron and a 9 mV shift for a two-electron oxidation at −70°C. Thus, the peak potential shift found in this study is seriously distorted by uncompensated resistance. Note that the overall reaction is of an ECE type, since the anodic peak current for the oxidation of the n-alkanes at an UME is greater than that expected for a one-electron reaction (and is closer to two) on the voltammetric time scale. In dilute solutions at the longer bulk electrolysis time scales, n_{app} was approximately two, while in more concentrated alkane solutions, n_{app} was larger than two.

Sigma electron delocalization in normal alkanes has previously been documented (23-27). ESR studies of singly oxidized extended chain hydrocarbons in frozen glasses at 4.2 K, generated by γ irradiation (in SF_6, chlorocarbon, and fluorocarbon solvents), clearly indicate delocalization of the unpaired electron over the entire chain. Characteristic 1:2:1 three-line spectra are observed. These are attributed to the strong, hyperfine coupling of the unpaired electrode in a σ-molecular orbital with the two end protons, which are in the plane of the alkane carbon-carbon bonds. A decrease in the coupling constant for the end protons with increasing number of carbons in the chain was attributed to the increasing σ delocalization. Comparison of the observed decrease in hyperfine coupling constants and anodic peak potential with hydrocarbon chain length is shown in Fig. 6.

Other examples of σ delocalization include studies of photoinduced electron transfers, between donor-acceptor molecules linked by hydrocarbon "spacers" (*i.e.*, electron transfer through-bond as well as through-space), which have been shown to be dependent on the spacer distance (28, 29). Sigma delocalization and σ-π interactions have been postulated to account for the observed large electron transfer rates. Electron and hole transfer rates obtained at donor (biphenyl)-acceptor (naphthalene) separations of *ca.* 15Å are about 400 times larger (28, 30) than the intramolecular electron (or hole) transfer rates of biphenyl and naphthalene in frozen glasses at the same average distance

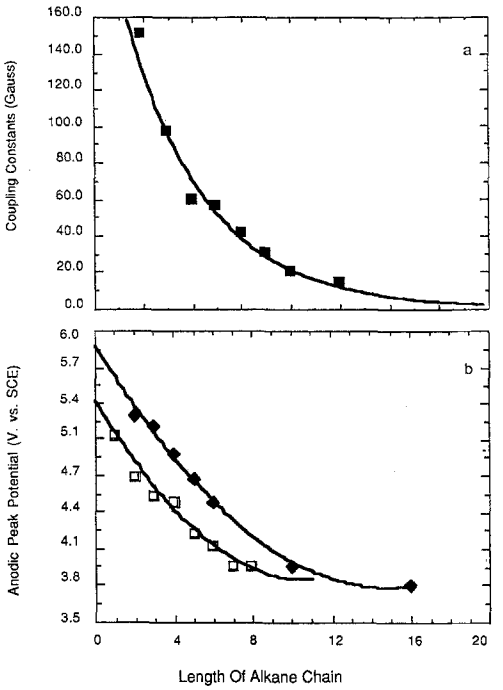

Fig. 6. (a) Correlation of ESR coupling constants for protons in the s in-plane orbital with length of hydrocarbon chain (23-27). (b) Correlation of anodic peak potentials for hydrocarbons and ammonium ions with length of hydrocarbon chain.

(31). The alkane linkage attenuates the decrease in electronic coupling (30) between the donor and acceptor molecules as a function of distance. Thus, the expected exponential decay with distance, as in tunneling through a single potential barrier, is not observed.

The peak potential shift observed for the oxidation of ammonium ions is similar to that of the n-alkanes and is also attributed to σ delocalization in the alkyl chain. The ammonium ion can be considered as a $-NR_3^+$-substituted hydrocarbon. This positively charged ($-NR_3^+$) substituent produces an electrostatic effect on the potential for oxidation, shifting it to more positive values. A 540 mV peak potential difference was observed between the oxidation of ethane (CH_3CH_2-H) and that of tetraethylammonium ion (CH_3CH_2-NR_3^+), Fig. 4. The electrostatic effect of the $-NR_3^+$ substituent decreased as the alkyl chain length increased, reaching a limit at about ten $-CH_2-$ groups. There was only a 10 mV difference between the anodic peak potential of octane and hexyltriethylammonium.

Conclusions

Electrochemical oxidation of normal saturated hydrocarbons and quaternary ammonium ions are possible in liquid $SO_2/CsAsF_6$. Irreversible voltammetric waves were observed for all compounds studied. The alkane voltammetric wave anodic peak currents suggest $n_{app} \geq 2$. For the alkylammonium voltammetric waves (Table V) $n_{app} \cong 1$ (cetyltrimethylammonium ion), 3 (decyltriethylammonium ion) and 5 (hexyltriethylammonium ion). A bulk electrolytic oxidation of the alkanes in dilute solutions occurred in a manner similar to that in previous reports (1-6), consuming two faradays per mole of alkane electrolyzed. The primary products formed in dilute solutions (*ca.* 1-10 m*M*) were shorter hydrocarbons. Electrolysis of concentrated alkane solutions may produce species that are oxidized at less positive potentials via reaction of the oxidation products with starting material (possibly leading to longer chain, branched, and unsaturated hydrocarbons), although oxidation of solvent or electrolyte may also take place.

The data presented here, in addition to those cited above, provide evidence for carbon σ-bond delocalization. Correlation of anodic peak potentials with gas-phase ionization potentials and calculated HOMO energies unambiguously show that useful electrochemical data can be obtained at potentials exceeding +5V *vs.* SCE. Because no significant background processes are observed up to +6V *vs.* SCE, yielding the largest available positive potential range reported to date, this system should prove useful in the study and generation of highly oxidized species. Because the solubility of the $CsAsF_6$ is low, *ca.* 30 m*M*, appreciable solution resistance is observed. This large solution resistance presents difficulties when fast scan rates or large electrodes are employed, but ultramicroelectrodes can be used to obtain useful voltammetric results. Because of interest in methane activation (32), the bulk electrolytic oxidation of methane and analysis of the product distribution should be the goal of future studies.

Acknowledgment

The support of this research by the National Science Foundation (CHE 8901450) is gratefully acknowledged.

Manuscript submitted Aug. 24, 1989; revised manuscript received March 19, 1990.

The University of Texas at Austin assisted in meeting the publication costs of this article.

REFERENCES

1. M. Fleishmann and D. Pletcher, *Tetrahedron Lett.*, **60,** 6255 (1968).
2. J. Bertram, M. Fleishmann, and D. Pletcher, *ibid.*, **4,** 349 (1971).
3. J. Bertram, J. P. Coleman, M. Fleishmann, and D. Pletcher, *J. Chem. Society Perkin II,* 374 (1973).
4. D. B. Clark, M. Fleishmann, and D. Pletcher, *ibid.*, 1578 (1973).
5. D. B. Clark, M. Fleishmann, and D. Pletcher, *J. Electroanal. Chem.*, **42,** 133 (1973).
6. J. P. Coleman and D. Pletcher, *Tetrahedron Lett.*, **2,** 147 (1974).
7. H. P. Fritz and T. Wurminghausen, *J. Electroanal. Chem.*, **54,** 181 (1974).
8. C. Pitti, F. Bobilliart, A. Thiebault, and M. Herlem, *Analyt. Lett.*, **8,** 241 (1975).
9. J. Cassidy, S. B. Khoo, and S. Pons, *J. Phys. Chem.*, **89,** 3933 (1985).
10. E. Garcia, J. Kwak, and A. J. Bard, *Inorg. Chem.*, **27,** 4377 (1988).
11. R. A. Malmsten, C. P. Smith, and H. S. White, *J. Electroanal. Chem.*, **215,** 223 (1986).
12. M. Fleishmann, S. Pons, D. Rolison, and P. P. Schmidt, "Ultramicroelectrodes," Datatech Science, Morganton, NC (1987).
13. J. O. Howell and R. M. Wightman, *Anal. Chem.*, **56,** 524 (1984).
14. J. O. Howell and R. M. Wightman, *J. Phys. Chem.*, **88,** 3915 (1984).
15. R. M. Wightman and D. O. Wipf, in "Electroanalytical Chemistry," Vol. 15, A. J. Bard, Editor, p. 249, Marcel Dekker, New York (1988).
16. C. R. Cabrera, E. Garcia, and A. J. Bard, *J. Electroanal. Chem.*, **260,** 457 (1989).
17. R. S. Nicholson and I. Shain, *Anal. Chem.*, **36,** 706 (1964).
18. R. S. Nicholson, *ibid.*, **37,** 1351 (1965).
19. (a) A. J. Bard and L. R. Faulkner, "Electrochemical Methods," Chap. 10, p. 379, John Wiley and Sons, New York (1980); (b) *ibid.*, Chap. 6, p. 222, and Chap. 11, p. 462.
20. E. Garcia and A. J. Bard, unpublished results: a diffusion coefficient of 3.3×10^{-6} has been obtained for the first oxidation of anthracene ($An/An^{+}\cdot$) in 0.2*M* $TBAAsF_6/SO_2$ at a 25 μm Pt UME at −70°C.
21. K. Shelly and C. A. Reed, *J. Am. Chem. Soc.*, **108,** 3117 (1986).
22. (a) A. Streitwiser, "Molecular Orbital Theory for Organic Chemists," Chap. 7, p. 186 and 199, John Wiley and Sons, New York (1961); (b) M. Peover, in "Electroanalytical Chemistry," Vol. 2, A. J. Bard, Editor, p. 35, Marcel Dekker, New York (1967).
23. K. Toriyama, K. Numome, and I. Machio, *J. Phys. Chem.*, **85,** 2149 (1981).
24. K. Toriyama, K. Numome, and I. Machio, *ibid.*, **77,** 5891 (1982).
25. K. Toriyama, K. Numome, and I. Machio, *ibid.*, **79,** 2499 (1983).
26. K. Toriyama, K. Numome, and I. Machio, *ibid., Fara-*

day Discuss. Chem. Soc., **78,** 19 (1984).
27. K. Toriyama, K. Numome, and I. Machio, *J. Phys. Chem.*, **90,** 6836 (1986).
28. K. Q. Penfield, J. R. Miller, M. N. Paddon-Row, E. Cotsaris, A. M. Oliver, and N. S. Hush, *J. Am. Chem. Soc.*, **109,** 5061 (1987).
29. H. Oevering, M. N. Paddon-Row, M. Heppener, A. M. Oliver, E. Cotsaris, J. W. Verhoeven, and N. S. Hush, *ibid.*, **109,** 3258 (1987).
30. M. D. Johnson, J. R. Miller, N. S. Green, and G. L. Closs, *J. Phys. Chem.*, **93,** 1173 (1989).
31. J. R. Miller, J. V. Beitz, and R. K. Huddleston, *J. Am. Chem. Soc.*, **109,** 5057 (1987).
32. H. Mimoun, *New J. Chem.*, **11,** 513 (1987).

Electronic State Densities of Ferrocene and Anthracene in Nonaqueous Solvents Determined by Electrochemical Tunneling Spectroscopy

H. Morisaki, A. Nishikawa, H. Ono, and K. Yazawa

The University of Electro-Communications, Chofu-shi, Tokyo 182, Japan

ABSTRACT

One-electron oxidations of ferrocene and anthracene to the corresponding radical cations have been used as model systems for studying solvent effects in heterogeneous charge-transfer kinetics. The energy dependencies of the electronic state densities of the reactants in several nonaqueous solvents have been investigated. The energy dependence of the state density of anthracene has shown a gaussian-shaped distribution function, whereas that of ferrocene has shown nongaussian distribution characterized by two reorganization energies. In the latter case, the reorganization energy corresponding to the main peak of the distribution function has been found to be correlated with the donor numer of the solvents, indicating the presence of a new inner-shell reorganization based on the donor-acceptor interaction. The two types of reorganization processes have been attributed to the solvation sites peculiar to the shape of the ferrocene molecule.

The electrochemical charge transfer at an electrode-electrolyte interface is strongly dependent upon various interactions between the electroactive species (donor or acceptor) and the surrounding solvents. This means that an analytical method for determining the electrochemical charge transfer may also become a useful tool for studying the solvent effects of ionic species or molecules. In previous reports, we have shown that the reorganization energy of several electroactive species in aqueous electrolytes can be determined unambiguously from a newly developed analytical method named electrochemical tunneling spectroscopy (1-3). In the present study, this technique is further utilized for studying solvent effects on the heterogeneous charge-transfer kinetics in nonaqueous electrolytes. The role of solvent reorganization dynamics in electron-transfer processes both in electrochemical and homogeneous systems has been the focus of many recent theoretical and experimental studies (4-10).

Concept of the Electronic State Density

Consider an anodic reaction as an example. The anodic current of a metal electrode in an electrolyte is given by

$$j_a(V) = eC \int k(E, V)N(E)[1 - f(E)]dE \quad [1]$$

where C is the concentration of reactants, $k(E, V)$ is the rate constant of the reaction which is a function of the polarization, $N(E)$ is the electronic state density in the metal electrode, and $f(E)$ is the Fermi-Dirac distribution function.

An alternative expression for the current at a solid-electrolyte interface is a representation similar to Eq. [1] except that the rate constant $k(E, V)$ is replaced by an electronic state density of reactants in the electrolyte, $D_{red}(E, V)$. The latter expression means that the anodic current is in proportion to the overlap integral between the vacant states in the metal electrode and the occupied states in the electrolyte. In other words, the rate constant, $k(E, V)$, is practically equivalent to the electronic state density, $D_{red}(E, V)$.

According to classical Marcus theory (11), the polarization-dependent electronic state density is given by

$$D_{red} = A \exp\left(-\frac{\Delta G^*}{kT}\right) \quad [2]$$

where

$$\Delta G^* = [\lambda + e(V - V^\circ)]^2/4\lambda \quad [3]$$

Here, λ and V are the reorganization energy and the formal redox potential of the redox couples, respectively, with the other symbols having their usual meanings.

The shape of the polarization dependence of the distribution function is a displaced gaussian with a maximum value at

$$|V - V^\circ| = \lambda/e \quad [4]$$

The main purpose of our experimental study series (1-3) is to elucidate the actual shape of the distribution functions in various electrolytes.

Experimental

The experimental technique and the theoretical background of the present study have been previously reported (1-3). The working electrode used in the present study is an oxide-covered Pt-silicide formed on n-type Si. The significance of using this type of electrode has been discussed elsewhere (2). The electroactive species used as the model system in the present experiment was mostly ferrocene [$Fe(Cp)_2$], although some experiments were made using anthracene (AN) and some other redox couples. Some of the reasons for this preferential use are as follows: Firstly $Fe(CP)_2$ dissolves in various organic solvents. Secondly, it has moderate redox potentials in most of the solvents; in the case of AN, the formal redox potential was inconveniently close to the anodic limit of the polarization window for most of the solvents.

Organic solvents used in the present experiment as well as their solvent parameters are listed in Table I. The ferrocene (or anthracene) concentration in such solvent was set in the range between 1 and 10 mM. A supporting electrolyte dissolved into each solvent was tetrabutylammonium perchlorate (TBAP). The concentration of TBAP was 0.1M. All chemicals were analytical grade and were used without further purification. Electrochemical measurements were carried out with the solutions under a nitrogen atmosphere. All electrode potentials were measured *vs.* an aqueous saturated calomel electrode (SCE) through a glass